

Glow-Peak Stability in $^6\text{LiF:Mg,Ti}$ (TLD-600) Exposed to a Fe-ion beam

HIROSHI YASUDA^{1*}

¹National Institute of Radiological Sciences Anagawa, Inage-ku, Chiba 263–8555, Japan

(Received, September 11, 2000)

(Revision received, December 6, 2000)

(Accepted, January 22, 2001)

thermoluminescent detector/ $^6\text{LiF:Mg,Ti}$ /glow curve deconvolution/annealing/NIRS-HIMAC

The stability of glow peaks in $^6\text{LiF:Mg,Ti}$ (TLD-600) exposed to a high-energy Fe-ion beam was examined in comparison to ^{137}Cs γ -ray irradiation under changing annealing conditions. The peak areas induced by the Fe ions were much smaller than those by γ -rays. The sizes and positions of peaks 3–5 in Fe-ion irradiated samples were hardly changed after post-annealing at $100^\circ\text{C} \times 30$ min, regardless of the pre-annealing conditions (fast quenching or subsequent pre-annealing at $100^\circ\text{C} \times 2$ h). Whereas, the peaks in γ -ray irradiated samples were notably affected by post-annealing; the peak positions and peak-area sizes changed in different ways depending on the pre-annealing conditions. The effects of post-annealing on peak 6 were identical for Fe ions and γ -rays. These facts suggest that peaks 3–5 in TLD-600 comprised both stable and unstable luminescent centers, and that the latter part would be easily depleted in highly dense ionization.

INTRODUCTION

The shapes of glow curves in $^6\text{LiF:Mg,Ti}$ (TLD-100/600/700) exposed to low-energy neutrons and heavy charged particles (HCP) are different from those to photons and electrons¹⁾. This feature has been utilized for discriminating doses from different-quality radiations in mixed fields^{2–9)} because of the advantages with regard to small-scale and simplicity in handling. Most of the previous studies relied on the TL ratio of the main dosimetric peak (peak 5) to the high-temperature peak (peak 7) of $^6\text{LiF:Mg,Ti}$, because of the contrasting responses to high-LET radiation and the easy technique for separating the two glow peaks. However, the use of peak 7 often suffers from the thermal noises inevitably occurring at such a high temperature. For this reason, peak 7 is thought to be inappropriate for low-dose measurements below ~ 2 mGy of γ -rays¹⁰⁾. In addition, Horowitz¹¹⁾ found the dependence of the peak-7 supralinearity on the photon energy. Thus, Yossian and Horowitz¹²⁾ have proposed using peak 4 in place of peak 7 to determine the γ -ray dose in a neutron-mixed field. This technique is based on the fact that the neutron-induced intensity of peak 4 relative to peak 5 in $^6\text{LiF:Mg,Ti}$ (TLD-600) is much smaller than the γ -ray induced one. A change in the peak area ratio is attributable to different secondary charged par-

*Author for correspondence: Hiroshi Yasuda, Ph.D. Int. Space Radiation Laboratory National Institute of Radiological Sciences 4–9–1 Anagawa, Inage-ku Chiba 263–8555, Japan.

Phone; +81-(0)43–251–2111 ex.6927, Fax; +81-(0)43–251–4531, E-mail; h_yasuda@nirs.go.jp

ticles, that is, alpha particles ($\text{LET}_{\infty} \cdot \text{H}_2\text{O} = 162 \sim 230 \text{ keV } \mu\text{m}^{-1}$) with tritium produced by neutrons and Compton electrons ($\text{LET}_{\infty} \cdot \text{H}_2\text{O} < 0.5 \text{ keV } \mu\text{m}^{-1}$) emitted by γ -rays. Accordingly, the peak-4 luminescent centers are assumed to be susceptible to dense energy absorption. If this assumption is correct, the peak-4 intensity relative to the other peaks should also be small for other heavy ions with a LET comparable to that of the alpha particles. Moreover, the instability of peak 4 may also be observed for thermal-energy absorption after irradiation, i.e. post-annealing.

MATERIALS AND METHODS

Polycrystalline chips of $^6\text{LiF:Mg,Ti}$ (TLD-600, HARSHAW) with dimensions of $3.2 \times 3.2 \times 0.9 \text{ mm}^3$ were employed in the present study. All of the TLD chips were taken from the same batch and tested for uniformity ($< 5\%$) in TL response using ^{137}Cs γ -rays at a dose level of 100 mGy for water. They were pre-annealed at $400^\circ\text{C} \times 1\text{h}$. Half of the chips were followed by a fast quench to room temperature in air. The other half were subsequently pre-annealed at $100^\circ\text{C} \times 1\text{h}$ and quenched naturally in air. It is known that the pre-annealing conditions affect the glow-curve shapes of LiF:Mg,Ti^{11} .

Two chips of TLD-600 were packed in a rectangular case of tissue-equivalent resin (Toughwater phantom, Kyotokagaku) with dimensions of $80 \times 80 \times 6 \text{ mm}^3$ including a 2 mm-thick cover. The TLD chips were exposed to a high-energy Fe-ion beam at the Biology room of NIRS-HIMAC and γ -rays from the NIRS ^{137}Cs source. One package received one of three dose levels: 10, 50, and 100 mGy for water; those were measured with an air-filled ion chamber calibrated to standard radiation sources. The uniformity of the Fe-ion beam at the target position with dimensions of $100 \times 100 \text{ mm}^2$ was confirmed using plastic nuclear track detectors (CR-39) and a beam-profile monitor installed in the beam line. The energy of the Fe ion ($Z = 26$, $A = 56$) was 500 MeV amu^{-1} at the beam exit and 440 MeV amu^{-1} at the target position. The unrestricted LET for water ($\text{LET}_{\infty} \cdot \text{H}_2\text{O}$, abbreviated to LET in the following) was calculated to be 197 keV mm^{-1} . This LET value is comparable to those of the alpha particles ($E = 2.05 \text{ MeV}$, $\text{LET} = 160 \sim 230 \text{ keV } \mu\text{m}^{-1}$) from the neutron-capture reaction in TLD-600: $^6\text{Li(n},\alpha)^3\text{H}^{13}$. The change in the LET inside a single chip (0.9 mm in thickness) was estimated to be less than 2%.

The next day after irradiation, half of the samples were post-annealed at $100^\circ\text{C} \times 30 \text{ min}$ for each pre-annealing condition. Consequently, four different annealing conditions were given, as shown in Table 1: fast quenching (A1), fast quenching + post-annealing (A2), subsequent pre-annealing (B1), and subsequent pre-annealing + post-annealing (B2). The thermoluminescence (TL) from the irradiated samples were read out two days after irradiation with an automatic TLD reader (HARSHAW Model 5500); those were heated to 360°C at a rate of 10°C s^{-1} . The TL readouts were automatically recorded as a function of the temperature on a personal computer.

Table 1. Conditions for annealing of the dosimeters. They were followed by fast quench in air.

	Pre-annealing	Post-annealing
A1	$400^\circ\text{C} \times 1 \text{ h}$	—
A2	$400^\circ\text{C} \times 1 \text{ h}$	$100^\circ\text{C} \times 30 \text{ min.}$
B1	$400^\circ\text{C} \times 1 \text{ h} + 100^\circ\text{C} \times 2 \text{ h}$	—
B2	$400^\circ\text{C} \times 1 \text{ h} + 100^\circ\text{C} \times 2 \text{ h}$	$100^\circ\text{C} \times 30 \text{ min.}$

RESULTS AND DISCUSSION

Dose-normalized glow curves of TLD-600 exposed to Fe-ion beam and ^{137}Cs γ -rays are shown in Fig. 1 versus the reader-indicated values of temperature; they are not exactly the averages in the chips. The glow curves are plotted separately in Fig. 1 for each annealing condition. The upper figures (Fig. 1a) were obtained for Fe ions and the lower figures (Fig. 1b) for γ -rays. Each plot is an average of the TL readouts from six chips (two chips at each of the three dose levels), since the dose-normalized glow-curves were nearly identical, irrespective of the delivered doses. The fast-quenched samples (A1 and A2) showed higher TL intensities than the subsequently pre-annealed samples (B1 and B2). These findings agree with the previous results that the TL intensity of LiF:Mg,Ti increases with increasing cooling rates^{11,14}. The glow-curve shapes of subsequently pre-annealed samples were smoother than those of fast-quenched samples for both Fe-ion and γ -ray irradiation. The effects of post-annealing were scarcely seen on the Fe-ion induced glow curves (Fig. 1a); identical shapes were observed for the different pre-annealing conditions. In contrast, the γ -ray induced glow curves showed notable changes after post-annealing (Fig. 1b).

The glow curves were deconvoluted to four major peaks (peaks 3–6), as shown in Fig. 1, using the Podgorsak-Moran-Cameron (PMC) approximation method¹⁵. This method is one of the popular techniques of computerized glow-curve deconvolution (CGCD) and the most efficient regarding to computer time¹⁶. Perks and Marshall⁶ have pointed out that the fits to a ^7LiF glow curve by means of the PMC method are identical to those with a more rigorous method of the Randall-Wilkins approximation to first-order kinetics¹⁷. The goodness of the fits was evaluated with the index of “figure of merit (FOM)”¹⁸, which is defined by

$$\text{FOM}(\%) = \sum_i^n \frac{100 \times |y_i - Y_i|}{A}, \quad (1)$$

where i is the number of a channel; n is the total number of channels; y_i is the measured TL intensity in channel- i ; Y_i is the value of a fitting function in channel- i ; and A is the total TL integral of the fitted glow curve over all channels. Less than 3% of the FOM was established for all cases (See Fig. 1) without the other small peaks employed by Yossian and Horowitz¹².

As shown in Fig. 1a, the glow peaks in the Fe-ion irradiated samples were hardly affected by post-annealing; only peak 6 of the subsequently pre-annealed samples increased. In contrast, the γ -ray induced peaks of the subsequently pre-annealed samples were notably pronounced by post-annealing (Fig. 1b). The relative area size of peak 3 or peak 4 normalized to peak 5 was considerably larger in the fast-quenched samples than in the subsequently pre-annealed ones. In a comparison for different quality radiations, the ratio of peak 3 or peak 4 to peak 5 in the fast-quenched samples were much smaller for Fe ions than those for γ -rays. These data agree with the CGCD results obtained by Yossian and Horowitz¹², in which the relative peak-4 intensity for $^6\text{LiF:Mg,Ti}$ normalized to peak 5 was much smaller for neutrons than that for ^{60}Co γ -rays. In subsequently pre-annealed samples, notable increases in the relative peak intensities after post-annealing were observed only for γ -ray irradiation.

The TL integrals of the deconvoluted glow-peak areas are summarized in Table 2. It can be seen that the Fe-ion induced peaks were smaller by 60–80% than the γ -ray induced peaks, except for peak 6 of the fast-quenched samples. Such reductions in the TL efficiency for heavy ions may be attributed to saturation of the luminescent centers, according to the fact that similar phenomena have also been

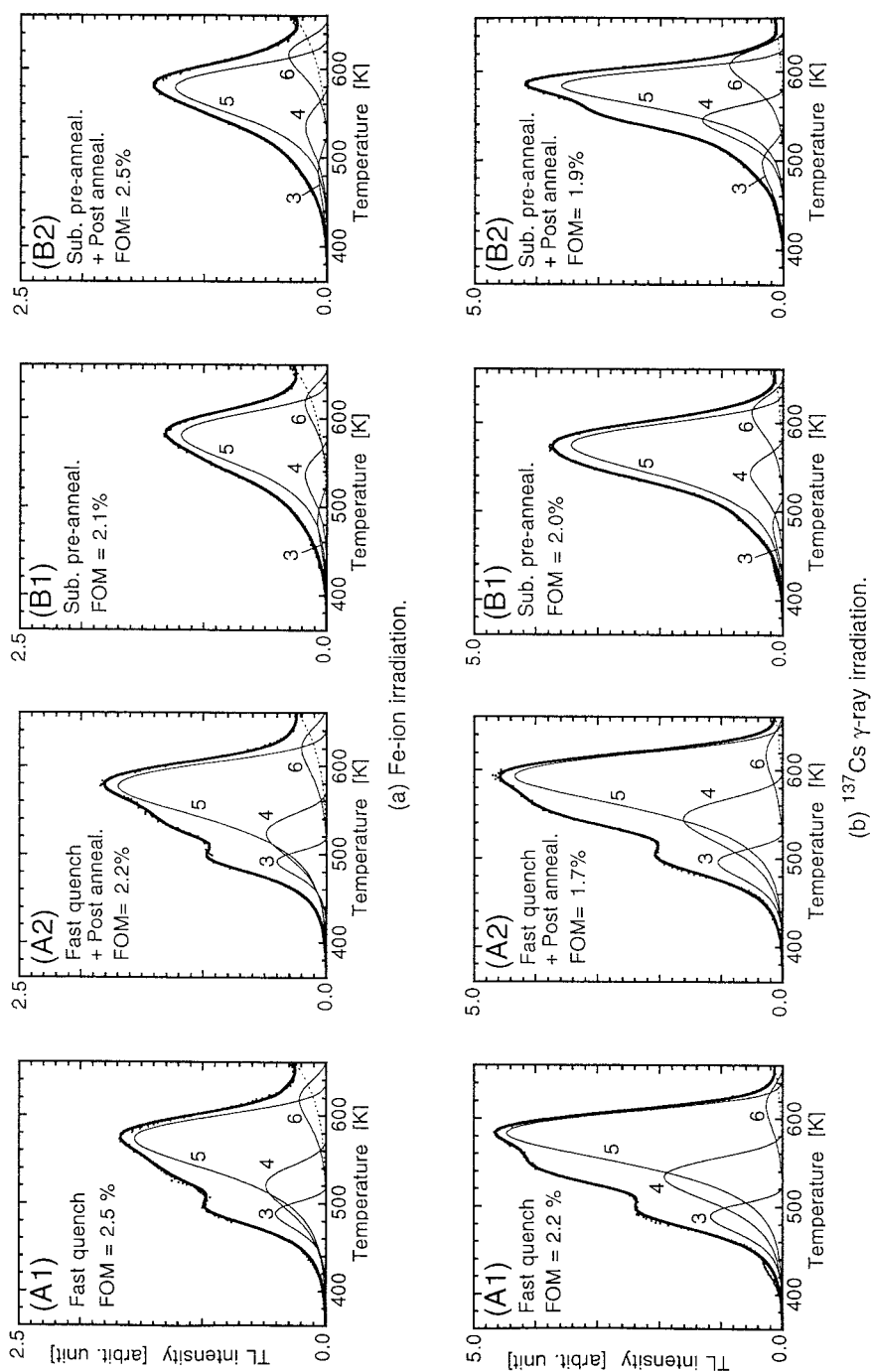


Fig. 1. Dose-normalized glow curves of TLD-600 exposed to 10, 50, and 100 mGy for water; these are grouped by the annealing conditions (see Table 1). The above figures (a) were obtained for high-energy Fe ions and the below figures (b) for ^{137}Cs source γ -rays. The glow curves were deconvoluted to four major peaks (peaks 3–6) using the PMC approximation method¹⁵⁾. Note that the scales of the vertical axis of the upper figures (a) are half of those of the lower ones (b).

Table 2. TL integrals of peaks 3–6 in $^6\text{LiF:Mg,Ti}$ (TLD-600) exposed to Fe ions and ^{137}Cs γ -rays, grouped by the annealing conditions.

Annealing condition	Radiation	Relative TL integral*			
		Peak 3	Peak 4	Peak 5	Peak 6
A1: Fast quench	Fe-ion beam (a)	0.052	0.10	0.39	0.043
	^{137}Cs γ -rays (b)	0.16	0.39	1.00	0.053
	Ratio of (a)/(b)	0.32	0.26	0.39	0.81
A2: A1+post anneal.	Fe-ion beam (a)	0.045	0.098	0.42	0.042
	^{137}Cs γ -rays (b)	0.15	0.34	1.00	0.057
	Ratio of (a)/(b)	0.31	0.29	0.42	0.73
B1: Sub. pre-anneal.	Fe-ion beam (a)	0.017	0.033	0.28	0.031
	^{137}Cs γ -rays (b)	0.028	0.092	0.80	0.090
	Ratio of (a)/(b)	0.61	0.36	0.35	0.35
B2: B1+post anneal.	Fe-ion beam (a)	0.017	0.037	0.27	0.054
	^{137}Cs γ -rays (b)	0.067	0.19	0.61	0.15
	Ratio of (a)/(b)	0.26	0.19	0.44	0.37

* The values were normalized to the integral of peak-5 area of the γ -ray irradiated samples in the condition A1. The statistical errors (type A) for these average values are less than 10% of one standard deviation.

observed for high-dose photon irradiation^{19–21}). With an analytic calculation model²²), it is predicted that the absorbed dose in LiF along the path of a Fe ion with an energy of 500 MeV amu^{-1} is extremely high ($> 1,000$ kGy) on the nanometer scale. This dose level corresponds to a temperature greater than 400°C for LiF (heat capacity: 41.6 J mol^{-1} K $^{-1}$ at 298.15K). Under such highly localized energy deposition, the energy absorption to trapped electrons and holes would be less efficient. This mechanism has been successfully explained *a priori* by means of target-hit models on the basis of the track-structure theory^{19,23–27}).

The effects of post-annealing on the peak positions were also examined for deconvoluted peaks 3–6. The glow curves of those peaks are shown in Figs. 2 and 3, being separated by the pre-annealing condition; the data for groups A1 and A2 (fast-quenched samples) are shown in Fig. 2 and those of the groups B1 and B2 (subsequently pre-annealed samples) in Fig. 3. We can see that the positions and sizes of Fe-ion induced peaks (Figs. 2a and 3a) were so resistant to post-annealing. Only the peak 6 of the subsequently pre-annealed samples showed a considerable change. In contrast, the γ -ray induced peaks were very vulnerable to the post-annealing; peaks 3–5 notably shifted to a higher temperature ranges. Also, the shapes of the γ -ray induced peaks considerably changed after post-annealing. Peaks 3 and 4 of the subsequent pre-annealed samples were pronounced (Fig. 3b) relative to the fast-quenched samples. Peak 5 of the subsequent pre-annealed samples became pointed (Fig. 3b). Peak 6 kept a stable position, as can also be seen for the Fe-ion irradiation.

The results obtained in the present study suggest that the luminescent centers of peaks 3–5 in TLD-600 are composed of at least two components having different stability. According to the results shown in Figs. 2 and 3, the γ -ray induced peaks would be accompanied by more unstable centers than the Fe-ion induced ones. The vulnerable feature of the γ -ray induced peaks agrees with the peak-4 instability observed during long storage^{28,29}). The stable feature of the Fe-ion induced peaks indicates that a large

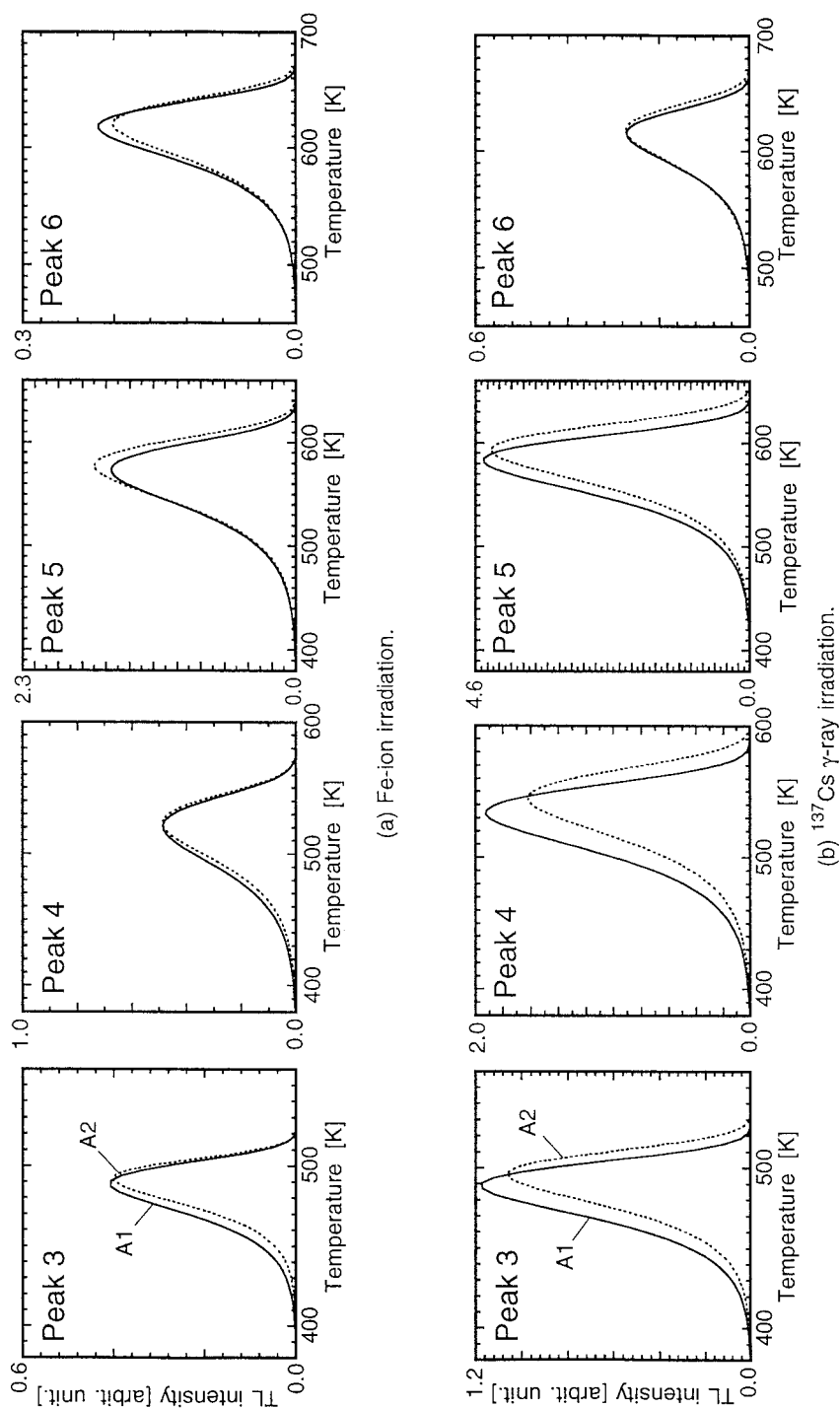


Fig. 2. Effects of post-annealing on glow peaks 3-6 of the fast-quenched TLD-600 exposed to Fe ions and ^{137}Cs γ -rays. Smoothed glow curves of group A1 and group A2 are indicated by the solid lines and the dotted ones, respectively. Note that the scales of the vertical axis of the upper figures (a) are half of those of the lower ones (b).

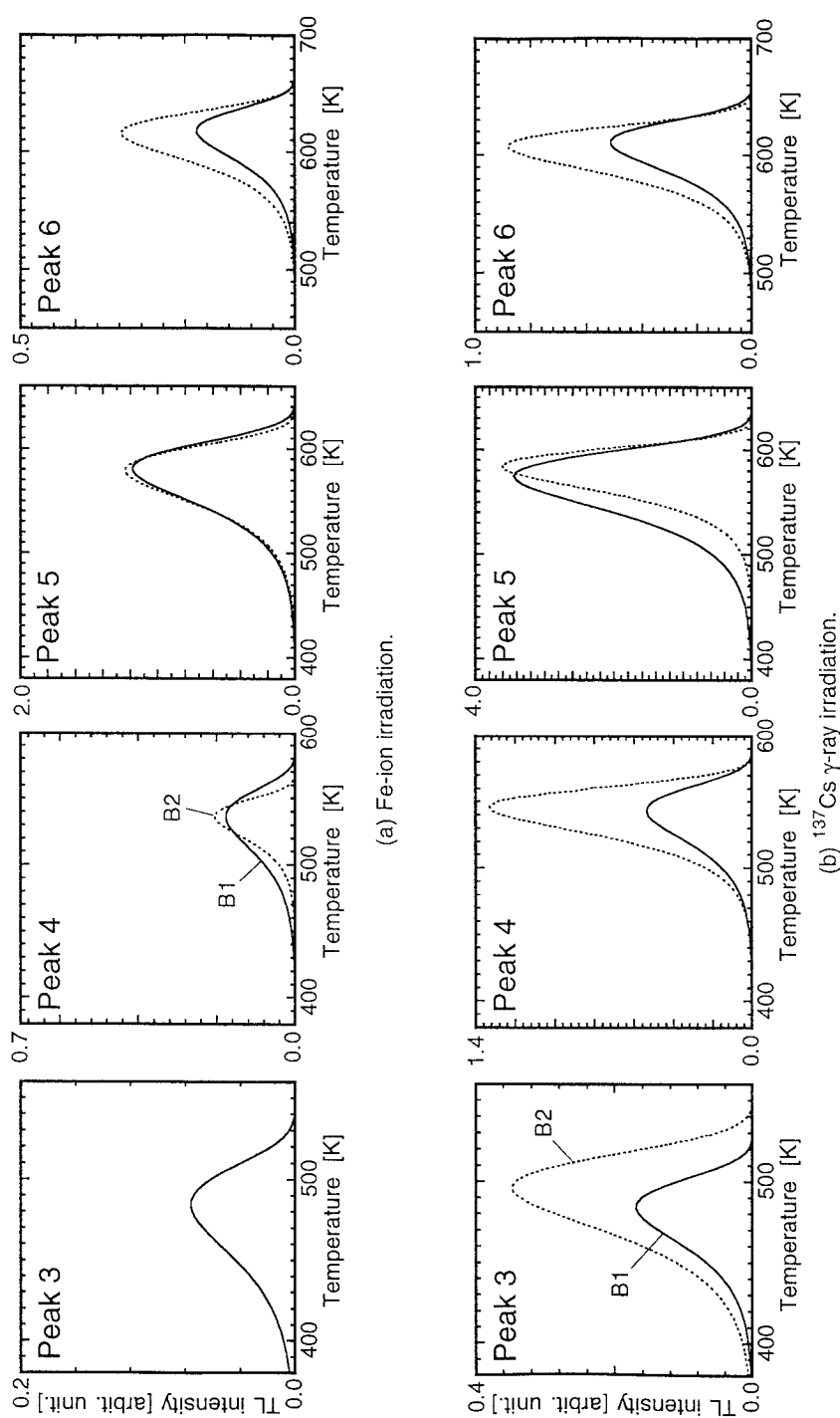


Fig. 3. Effects of post-annealing on glow peaks 3-6 of the subsequently pre-annealed TLD-600 exposed to Fe ions and ^{137}Cs γ -rays. Smoothed glow curves of the group B1 and the group B2 are indicated with the solid lines and the dotted ones, respectively. Note that the scales of the vertical axis of the upper figures (a) are half of those of the lower ones (b).

part of the unstable centers had already been depleted before reading. Dense energy absorption along the path of a heavy ion would act as local annealing for the luminescent centers of ${}^6\text{LiF:Mg,Ti}$.

The instability of the γ -ray induced peaks can be related to the instability of impurity-vacancy ($\text{Mg-Li}_{\text{vac}}$) dipoles. It is known that annealing at $400^\circ\text{C} \times 1\text{h}$ results in most of the Mg being in the form of $\text{Mg-Li}_{\text{vac}}$ dipoles, and subsequent annealing at 100°C establishes a new equilibrium of Mg present in the form of trimers³⁰⁾. Thus, a part of the γ -ray induced peaks in the fast quenched samples (Fig. 2) are possibly present with $\text{Mg-Li}_{\text{vac}}$ dipoles. The stable peak 6 is considered to be independent of the Mg-form changes. It is still unclear, however, why the γ -ray induced peaks were pronounced after post-annealing (Fig. 3) only for the subsequently pre-annealed samples. We hope to thoroughly explain the mechanism of such peculiar behaviors of glow peaks in LiF:Mg,Ti , and thus to confirm the reproducibility of the experimental results.

CONCLUSION

The glow-peak stability in TLD-600 appeared much differently for an energetic Fe-ion beam and ${}^{137}\text{Cs}$ source γ -rays. It was confirmed that the relative peak 4 intensity normalized to peak 5 was much smaller for Fe ions than for γ -rays, as expected from the previous data obtained for neutrons. In general, the glow peaks induced by γ -rays were more intense, but more vulnerable than the Fe-ion induced peaks. These results suggest that the luminescent centers of the major peaks in TLD600 are composed of both stable and vulnerable parts, and that most of the latter centers would be depleted under highly dense ionization.

The dependence of the glow-curve shapes on the radiation quality will be preferably implemented to dosimetry in neutron- or HCP-mixed fields. We may enhance the sizes, shapes, and positions of the glow peaks in TLD-600 by post-annealing to clearly discriminate TL signals from different quality radiations. With such an enhancing process, the method for evaluating the radiation quality using the peaks 4/5 ratio¹²⁾ would be more promising in a practical sense. It should be noted, however, that such techniques, depending on the vulnerable features of the low-temperature peaks, require rigorous handling of the dosimeters.

ACKNOWLEDGEMENTS

Sincere appreciation is expressed to Ms. Sayaka Sato, Tohoku Univ., for technical assistance. The Fe-ion exposure was carried out as part of the Research Project using Heavy Ions at NIRS-HIMAC.

REFERENCES

1. Horowitz, Y. S. and Yossian, D. (1995) Computerized glow curve deconvolution: application to thermoluminescent dosimetry. *Radiat. Prot. Dosim.* **60**: 1–102.
2. Burgkhardt, B. and Piesch, E. (1982) A computer assisted evaluation technique for albedo thermoluminescence dosimeters. *Radiat. Prot. Dosim.*, **2**: 221–230.
3. Hoffman, W. and Prediger, B. (1984) Heavy particle dosimetry with high temperature peaks of $\text{CaF}_2:\text{Tm}$ and ${}^7\text{LiF}$ phosphors. *Radiat. Prot. Dosim.* **6**: 149–152.

4. Meissner, P., Beinek, U., and Rassow, J. (1988) Applicability of TLD-700 detectors for dosimetry in d(14) + Be neutrons fields. *Radiat. Prot. Dosim.* **23**: 421–424.
5. Horowitz, Y. S. and Schachar, B. B. (1990) Sensitized TLD-700 for neutron-gamma dosimetry at radiation protection dose levels. *Radiat. Prot. Dosim.* **33**: 263–266.
6. Perks, C. A., and Marshall, M. (1991) Techniques for thermoluminescence glow curve analysis. *Radiat. Prot. Dosim.* **38**: 261–69.
7. Horiuchi, N. and Sato, T. (1992) Simultaneous evaluation of the neutron and gamma dose with a single ^6LiF TLD. *Nucl. Instrum. Meth.* **A317**: 545–552.
8. Piters, T. M., Bos, A. J. J. and Zoetelief, J. (1992) Thermoluminescence dosimetry in mixed neutron-gamma radiation fields using glow curve superposition. *Radiat. Prot. Dosim.* **44**: 305–308.
9. Vana, N., Schoner, W., Fugger, M., and Akatov, Y. (1996) Absorbed dose measurement and LET determination with TLDs in space. *Radiat. Prot. Dosim.* **66**: 145–152.
10. Schachar, B. B. and Horowitz, Y. S. (1988) Dosimetric characteristics of the high temperature peaks of LiF:Mg,Ti and $\text{CaF}_2\text{:Ti}$ using computerized glow curve deconvolution. *Radiat. Prot. Dosim.* **22**: 87–96.
11. Horowitz, Y. S. (1990) The annealing characteristics of LiF:Mg,Ti . *Radiat. Prot. Dosim.* **30**: 219–230.
12. Yossian, D. and Horowitz, Y. S. (1998) Estimation of gamma dose in neutron dosimetry using peak 4 to peak 5 ratios in LiF:Mg,Ti (TLD-100/600). *Radiat. Prot. Dosim.* **77**: 151–158.
13. Knoll, G. F. (1979) *Radiation Detection and Measurement* (2nd Edition). p.485, Wiley, New York.
14. Horowitz, Y. S., Mahajna, S., Oster, L., Weizman, Y., Satinger, D. and Yossian, D. (1998) The unified interaction model applied to the gamma-induced supralinearity and sensitisation of peaks 4 and 5 in LiF:Mg,Ti (TLD-100). *Radiat. Prot. Dosim.* **78**: 169–193.
15. Podgorsak, E. B., Moran, P. R., and Cameron, J. R. (1971) Interpretation of resolved glow curve shapes in LiF (TLD-100) from 100 K to 500 K. In : *Proc. 3rd Int. Conf. on Luminescence Dosimetry* (Denmark), Riso Report 249, p.1, IAEA/Danish AEC, Vienna.
16. Bos, A. J. J., Piters, T. M., Gomez Ros, J. M., and Delgado, A. (1993) An intercomparison of glow curve analysis computer programs: I. Synthetic glow curves. *Radiat. Prot. Dosim.* **47**: 473–477.
17. Randall, J. T. and Wilkins, M. H. F. (1945) Phosphorescence and electron traps. I. The study of trap distributions. *Proc. Roy. Soc.* **A184**: 366–389.
18. Balian, H. G. and Eddy, N. W. (1977) Figure of merit (FOM), an improved criterion over the normalized chi-squared test for assessing goodness-of-fit of gamma ray spectra peaks. *Nucl. Instrum. Meth.*, **145**: 389–395.
19. Moscovitch, M. and Horowitz, Y. S. (1988) A microdosimetric track structure model applied to alpha particle induced supralinearity and linearity in thermoluminescent LiF:Mg,Ti . *J. Phys. D.: Appl. Phys.* **21**: 804–814.
20. Horowitz, Y. S. and Yossian, D. (1995) Computerized glow curve deconvolution : application to thermoluminescence dosimetry. *Radiat. Prot. Dosim.* **60**: 1–102.
21. Chen, R. and McKeever, S. W. S. (1997) *Theory of thermoluminescence and related phenomena*. pp. 151–214, World Scientific, Singapore.
22. Katz, R., Loh, K. S., Daling, L., and Huang, G.-R. (1990) An analytic representation of the radial distribution of dose from energetic heavy ions in water, Si, LiF, NaI, and SiO_2 . *Radiat. Eff. Defects Solid.* **114**: 15–20.
23. Kalef-Ezra, J. and Horowitz, Y. S. (1982) Heavy charged particle thermoluminescence dosimetry: track structure theory and experiments. *Int. J. Appl. Radiat. Isot.* **33**: 1085–1100.
24. Daling, L. and Katz, R. (1991) Thindown in lithium fluoride (TL-100). *Nucl. Sci. Tech.* **2**: 147–152.
25. Olko, P., Bilski, P., and Michalik, V. M. (1994) Microdosimetric analysis of the response of LiF thermoluminescent detectors for radiations of different qualities. *Radiat. Prot. Dosim.* **52**: 405–408.
26. Geiss, O.B., Kramer, M., and Kraft, G. (1998) Efficiency of thermoluminescent detectors to heavy charged particles. *Nucl. Instrum. Meth.* **B142**: 592–598.
27. Avila, O., Gamboa-deBuen, I., and Brandan, M. E. (1999) Study of the energy deposition in LiF by heavy charged particle irradiation and its relation to the thermoluminescent efficiency of the material. *J. Phys. D: Appl. Phys.* **32**: 1175–1181.
28. Delgado, A. and Gomez Ros, J. M. (1990) Modifications induced in the TLD-100 trap distribution during expo-

- tures at different ambient temperatures. *Radiat. Prot. Dosim.* **34**: 233–235.
29. Delgado, A. Gomez Ros, J. M., Muniz, J. L., Bos, A. J. J., and Piers, T. M. (1993) Confirmation of the evolution of TLD-100 glow peaks 4 and 5 during storage at ambient temperatures. *Radiat. Prot. Dosim.* **47**, 231–234.
 30. McKeever, S. W. S., Moscovitch, M., Townsend, P. D. (1995) Thermoluminescence dosimetry materials: properties and uses. pp.45-202, Nuclear Technology Publishing, Ashford.